

Morphometry of the Samalayuca dunes, northern Chihuahua, Mexico

Morfometría de las dunas de Samalayuca, norte de Chihuahua, México

Miguel Domínguez-Acosta^{1*}, Richard P. Langford², Thomas E. Gill²

¹ Departamento de Ingeniería Civil y Ambiental, Universidad Autónoma de Ciudad Juárez, Ave. del Charro 450 norte, 32310, Ciudad Juárez, Chihuahua, Mexico

² Department of Earth, Environmental and Resource Sciences, The University of Texas at El Paso, 500 West University Avenue, 79968, El Paso, Texas, USA.

* Corresponding author: (M. Domínguez-Acosta) midoming@uacj.mx

How to cite this article:

Domínguez Acosta, M., Langford, R.P., Gill, T.E., 2023, Morphometry of the Samalayuca dunes, Northern Chihuahua, Mexico: Boletín de la Sociedad Geológica Mexicana, 75 (3), A240823. <http://dx.doi.org/10.18268/BSGM2023v75n3a240823>

Manuscript received: May 9, 2023.
Corrected manuscript received: August 13, 2023.
Manuscript accepted: August 22, 2023.

Peer Reviewing under the responsibility of Universidad Nacional Autónoma de México.

This is an open access article under the CC BY-NC-SA license (<https://creativecommons.org/licenses/by-nc-sa/4.0/>)

ABSTRACT

The Samalayuca Dunes (SMD) (Médanos de Samalayuca), Chihuahua, México, are one of México's largest and least studied dune fields, now managed as a Protected Area for their ecological characteristics. We present a morphometric characterization of the dune field based on remote sensing and field studies, to advance understanding of its physical environment. SMD's generally-fine sands originate from shoreline deposits of Paleolake Palomas, transported eastward (downwind) along an aeolian corridor, accumulating primarily as echo dunes upwind of the sierras of Samalayuca and Presidio. A complex wind regime, with northerly and southerly winds complementing regionally-prevailing southwesterlies, modified by topographic effects, shapes the SMD's morphology. The sand sea covers ~139.7 km², with ~113.8 km² in the main eastern body and ~25.9 km² in a northwestern subfield. We describe six major dune forms: north to south straight-crested dunes, east to west straight-crested dunes, star dunes, vegetated parabolic dunes, relict transverse dunes, and "megastar" (draa) dunes. Mean interdune centroid spacing is 76.5 m. The active dunes, previously described as an "aklé" pattern, are predominantly straight-crested dune sets oriented near-perpendicular to each other with general north-south and east-west crest orientations, 4-5 m high, spaced ~67 m apart for north-south trending crests and ~53 m for east-west trending crests, representing a nearly perpendicular interference pattern in some locations. The active dunes are superimposed in a compound and complex arrangement on relict remnants of much larger north-northwest trending transverse dune ridges fanning out from south to north-northwest, spaced approximately ~1 km apart and ~50 m high. The easternmost dune ridge contains an active set of at least 15 active megastar and reversing dunes up to 120 m tall, increasing in size and complexity from south to north. As a protected area with historical and ecological value, additional geologic investigations should be performed at the SMD, to help conserve this remarkable geologic feature.

Keywords: dunes, sand, aeolian processes, Samalayuca, Chihuahua.

RESUMEN

Las Dunas o Médanos de Samalayuca se localizan en el estado de Chihuahua, México, y forman parte de uno de los ergs más grandes y menos estudiados en México, y que actualmente se encuentran designadas como área de protección de flora y fauna. Este estudio presenta una caracterización morfométrica del campo de dunas, basada en datos de campo y sensores remotos, con la intención de establecer la base de entendimiento de este sistema. Sus sedimentos en tamaño de arenas finas tienen origen en los depósitos de litoral del Paleo-lago Pluvial Palomas, son transportados rumbo al este a través de un corredor eólico y depositados principalmente como dunas tipo eco en el margen oeste de las sierras de Samalayuca y del Presidio. Su morfología está influenciada por un régimen complejo de vientos provenientes del norte y del sur, los cuales complementan a los vientos prevalentes en la región provenientes del suroeste, además de los efectos topográficos impuestos por las sierras cercanas. Las dunas cubren una superficie de ~139.7 km², de las cuales, el cuerpo principal abarca ~113.8 km², mientras que el menor un área aproximada de ~25.9 km². Se describen seis tipos principales de dunas: dunas de crestas rectilíneas orientadas norte a sur, dunas de crestas rectilíneas orientadas este a oeste, dunas estrella, dunas parabólicas vegetadas, dunas transversales relictas y, dunas "megaestrella" o draa. El espaciamiento promedio del centroide de interdunas es de 76.5 m. Las dunas activas más abundantes están formadas por juegos de dunas rectilíneas, orientadas de forma cuasi-perpendicular entre ellas, con orientación general de crestas norte-sur y este-oeste, una altura promedio de 4 a 5 m y, un espaciamiento promedio de ~67 m para las crestas norte-sur y ~53 m para las crestas este-oeste. Estas dunas previamente descritas como "aklé", son en realidad resultado de un patrón de interferencia cuasi-perpendicular. Las dunas activas sobreyacen de forma compuesta y compleja a los remanentes relictos de cordilleras de megadunas transversales orientadas NNO, las cuales presentan un espaciamiento promedio de ~1 km y altura de ~50 m. La cordillera de mayor relieve presenta un grupo de aproximadamente 15 dunas activas de tipo megaestrella e inversas de hasta 120 m de altura, las cuales incrementan en tamaño y complejidad de sur a norte. Acorde con su estatus de área de protección ecológica y su gran valor geológico e histórico, es necesario continuar con la investigación que permita garantizar la preservación este imponente y bello monumento geológico.

Palabras clave: dunas, arena, procesos eólicos, Samalayuca, Chihuahua.

1. Introduction

Sand seas or ergs, representing sand dune systems with areas greater than 100 km², are the largest aeolian depositional landforms on Earth. They represent the primary depositional sink of aeolian sand transport systems, in which sediment is transported from source areas of a variety of types, along transport pathways or corridors, to sand seas and dune fields (Lancaster, 2022). Most sand seas show distinct spatial patterns of dune types as well as variations in dune morphometry, representing geomorphic expressions of the factors controlling their development through time (Ewing and Kocurek, 2010a; Lancaster, 2022). Ergs also tend to represent a mosaic of different generations of distinct groups of dunes, each formed in a different set of boundary conditions and sediment configuration (Lancaster, 1999). The accumulation of most terrestrial sand seas has taken place over periods of at least thousands of years, periods in which environmental changes during the Quaternary have had a significant effect on the supply, availability, and mobility of sand feeding and comprising the ergs (Lancaster, 2022).

The Samalayuca Dunes (SMD) (Médanos de Samalayuca) in northern Chihuahua, México (Figure 1) are one of the most iconic and beautiful geologic landmarks of the Chihuahuan Desert and one of the few sand seas in México. However, they have been one of the least studied.

Compared to the much more widely described and studied dune field of White Sands, New Mexico, USA (McKee, 1966, Ewing, 2020), some 150 km north of the SMD, the Samalayuca Dunes have had only a few scientific descriptions. The field is not designated on the Ciudad Juárez H13-1 El Porvenir H13-2 1:250,000 scale geologic map (Servicio Geológico Mexicano, 2003), where it is included as part of a large area of Quaternary aeolian sand. Webb (1969) stated, “the dunes do not appear to fit any conventional classification of dune forms, but are rather nondescript piles of sand with irregular and inconsistent shapes” anchored by irregular bedrock outcrops buried underneath

the sand. Reeves (1969) presented a brief mention of the dunes as the depocenter of saltating sands originating from Pluvial Lake Palomas. The most extensive prior description of the SMD was by Schmidt and Marston (1981), who proposed two distinct dune morphologies, an extensive “aklé” pattern and large “echo” dunes. Based on gravity and magnetic data, Schmidt and Marston (1981) proposed an aeolian-controlled dune-forming mechanism, instead of Webb’s (1969) basement control. Access to remote sensing imagery and additional field observations have led to a new morphometric and physical interpretation of the SMD field, which we present here.

In 2009 the Mexican government established the Médanos de Samalayuca, including the Sierra de Samalayuca, as an area for the protection of flora and fauna, due to the special ecological and environmental character of the dunes and surrounding sierras. The reason supporting this declaration, as stated in the Management Program (SEMARNAT, 2013), was the presence of unique and/or endemic species of flora and fauna, mainly in the dune area. It is clear that the preservation of native plants and animals is a laudable goal that should be pursued. Nevertheless, in order to achieve the preservation of any living species, a profound understanding of the physical environment that provides the basis of its ecosystem has to be clear and readily available to the decision makers, in order to accomplish the best policies possible. However, general knowledge of the physical geography and geology of the SMD, its source(s), formation, character, morphology, dynamics, and general behavior of the dunes has been largely lacking. This study aims to initiate the basis for the formal understanding of the SMD through the morphological characterization of the field and the description of its general formation dynamics as well as the general geomorphological context in which the SMD lies.

1.1. GEOGRAPHIC SETTING

The SMD are located in northern Chihuahua, México, in the northeastern Chihuahuan Desert,

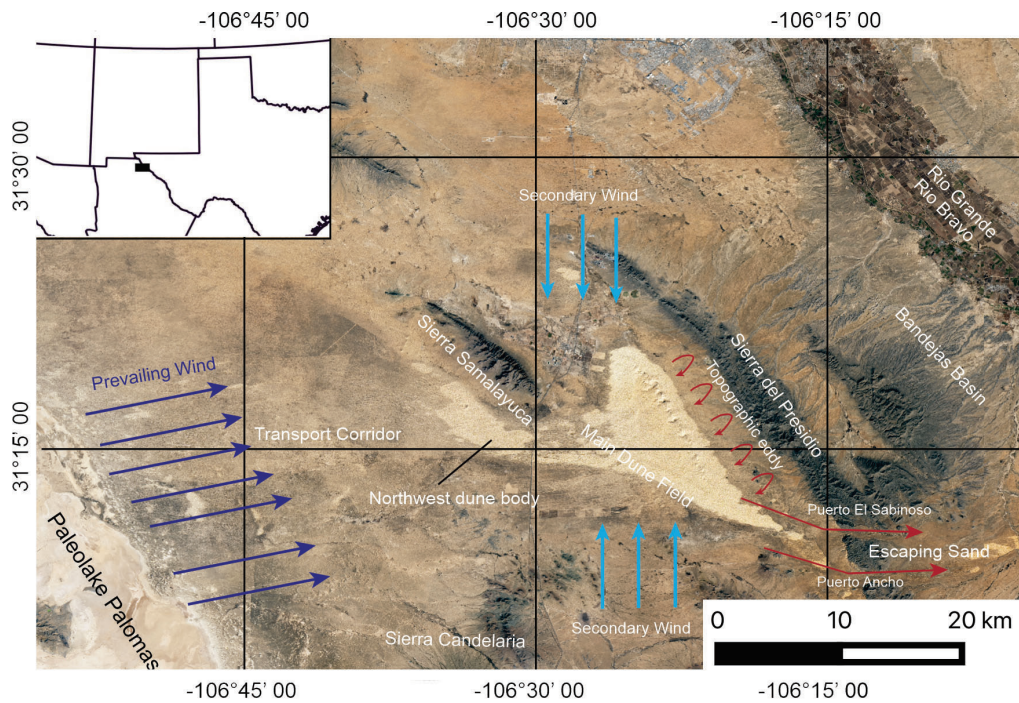


Figure 1 Regional location and physiographic setting of the Samalayuca dune field, northern Chihuahua, Mexico (center of the field approximately located at N 31° 15' 49", W 106° 23' 43"). Arrows show the conceptual wind regime. Dark blue arrows indicate the local prevailing westerly wind direction while lighter blue arrows indicate the secondary north and south directions. Red arrows indicate pathways of sand escaping through passes in the Sierra del Presidio and the presumed vortex that localizes the dune field. Inset, location of figure in SW North America. Image from Sentinel (ESA), April 28, 2023.

approximately 45 km south of the USA-México border (Figure 1). Located at approximately 31 degrees north latitude, the SMD is one of the southernmost sand seas in North America. The area experiences a cold arid climate (Köppen climatic classification BWk) with precipitation predominantly during the summer North American Monsoon. Average annual precipitation has been described as 212 mm (Schmidt and Marston, 1981; Garcia De la Peña *et al.*, 2012; Rueda-Torres *et al.*, 2022) to 252 mm (Villegas *et al.*, 1989). Although this region experiences strong winds, predominantly from the southwest during the dry season (November- May) and is part of a major Western Hemisphere aeolian dust emission region (Prospero *et al.*, 2002), the dune field itself is not a major source of dust (Baddock *et al.*, 2011).

Vegetation within the dune field is sparse, predominantly along its edges and within

interdunes, and is of typical xerophytic Chihuahuan Desert species including mesquite (*Prosopis glandulosa*), creosote bush (*Larrea tridentata*), and saltbush (*Atriplex canescens*) (García-De la Peña *et al.*, 2012; Rueda-Torres *et al.*, 2022). However, as with other dune environments, an increased number of endemic species, for example, the cactus *Echinocereus pectinatus*, are described (Enriquez Anchondo, 2003).

The immediate area of the SMD has a low human population density. It is part of the municipality of Ciudad Juárez, Chihuahua, the major population center, approximately 45 km north of the dune field. The nearest human settlement to the dunes, the town of Samalayuca, approximately 5 km west of the closest portion of the SMD, had a 2020 population of 1,577 inhabitants (Cervantes-Rendón *et al.*, 2022).

1.2. GEOLOGICAL SETTING

The Samalayuca Dune field sits on a Late Paleogene extensional basin of the Mexican Highlands section of the Basin and Range physiographic province, characterized by continuous NNW-trending mountain ranges intercalated by flat, low-lying basins (Reeves, 1969; Hawley *et al.*, 2000; Kennedy and Hawley, 2003). The SMD is flanked to the ENE by Cretaceous limestones of the Sierra del Presidio (maximum elevation ~1820 m amsl) (INEGI, 1983; Servicio Geológico Mexicano, 2003) and partially metamorphosed clastic sediments of the Sierra de Samalayuca (maximum elevation >1700 m amsl) of probable Triassic and Jurassic age (INEGI, 1983; Lawton *et al.*, 2018). Approximately 6 km to the south, the SMD is flanked by a few small Quaternary basalt and Cretaceous limestone outcrops of the Cerros la Morita. Further south (~4 km) outcrop the Paleogene intrusives of the Cerros las Felipas and the Sierra las Conchas (Servicio Geológico Mexicano, 2003). Approximately 13 km south from the SMD is the very prominent Sierra Candelaria (maximum elevation ~1900 m amsl), formed by Paleogene intrusives (INEGI, 1983; Servicio Geológico Mexicano, 2003). The sierras of Samalayuca, Presidio and Candelaria along with, to a lesser extent, the other above mentioned ranges form barriers to the prevailing wind, influencing the formation and shape of the SMD (Figure 1).

The SMD rise from the southeastern corner of an extensive sand sheet (total area >4700 km²) extending northwards into south-central New Mexico, USA (Hall and Goble, 2015). Much of the rest of the sand sheet is covered by mesquite coppice dunes (nabkhas) (Langford, 2000). Upwind (west) from the SMD lies an aeolian transport corridor extending ~40 km (Dominguez Acosta *et al.*, 2006; Dominguez Acosta, 2009). The aeolian corridor sits atop a gentle west-sloping surface formed by a series of alluvial fans and localized flat, low-lying desert playa surfaces. These surfaces are scattered throughout the corridor and are only

exposed along the cuts of ephemeral streams (arroyos) and within the playas themselves. Almost all of the aeolian corridor is covered by the thin (~3 m thick) sand sheet overlaid in most areas by extensive nabkha fields and scattered active dunes. The corridor's dune forms include barchan and barchanoid ridges as well as parabolic dunes (Dominguez Acosta, 2009). The western margin of the corridor is defined by the boundary with the ~200 km long (NNW to SSE) and >27 km wide (E to W) Pleistocene Pluvial Lake (Paleolake) Palomas (PLP) (Reeves, 1969; Kennedy and Hawley, 2003; Scuderi *et al.*, 2010). The lacustrine shoreline sand deposits of the PLP are interpreted as the source sediments for the sands extending across the corridor and to their ultimate deposition in the SMD (Reeves, 1969; Schmidt and Marston, 1981; Dominguez Acosta and Gill, 2007) (Figure 1). The SMD, tens of kilometers from the inferred sand source at PLP, represent a dry aeolian system in the classification scheme described in Lancaster (2022).

1.3. THE DUNE FIELD

The SMD, excluding the extensive and largely vegetated surrounding sand sheet and nabkha fields (Hall and Goble, 2015; Langford, 2000), can be best described as two connected bodies of active dunes (Figure 1). The main body of dunes is located the furthest downwind, adjacent to the Sierra del Presidio, it elongates to the NNW, and is approximately 24 km long and 15 km at its widest point. The eastern (downwind) margin of the main body of dunes is parallel to the western (upwind) side of the Sierra del Presidio and maintains an almost constant distance of approximately 4 km from the active sand margin to the base of the mountain range. The second and smaller body of dunes is located upwind (west) from the main body, adjacent to the Sierra de Samalayuca, and is approximately 9 km long to the NNW direction and approximately 6.5 km wide from west to east at its widest point. This western field maintains an approximate distance of 2 to 2.5 km

from the downwind margin of active sand to the southwestern margin of the Sierra de Samalayuca.

Aeolian transport of sand across the corridor and into the dunes is locally achieved by the presence of a multi-directional wind pattern derived from the interaction of the prevailing regional southwesterly winds and the (seasonal) variable wind directions from the north and south (Schmidt and Marston, 1981). The prevailing wind vectors are likely deflected by the topographical highs created by the sierras de Samalayuca and Candelaria upwind from the SMD. The Sierra de Samalayuca deflects the prevailing SW wind around it to the south, while the sierras de la Candelaria and Las Conchas similarly deflect the wind around them (Figure 1). The SMD exhibit a funnel shape, expanding from this gap into the main SMD area, which is likely due to the deflections caused by these ranges (Figure 1).

The Sierra del Presidio, downwind of the SMD, plays a prime role in the dune field's formation as sands accumulate close to the upwind side of this mountain range at a constant distance of approximately 4 km. This effect is achieved by the decrease in wind competence as airflow is forced to rise in order to cross the summit at ~1820 m amsl that forms almost 600 m of relief from the surrounding basin surface (~1250 m amsl) (INEGI, 1983). The Sierra del Presidio also clearly plays an important role in the location of the downwind SMD margin and the formation of some of the easternmost and larger dune forms in the field, possibly by creating a reversing (eddy like) wind flow, which is deflected back from the NE towards the SMD (Figure 1).

At the southernmost part of the erg, there are two gaps in the Sierra del Presidio known as Puerto El Sabinoso and Puerto Ancho (from north to south) that serve as escape routes for the SMD sediments (Figure 1). The exiting sediments accumulate downwind in the Bandejas Basin at the margin with the Bandejas Arroyo, forming a small ~5 km long (west to east) and ~1 to 1.5 km wide dune field (Figure 1). The sand escaped from the main dune field and accumulating at this site

may then be transported downwind by aeolian action along the western-northern margin of the Sierra de San Ignacio (maximum elevation >1780 m amsl). Some of these sands are ultimately removed from the aeolian system and transported downstream by fluvial action along the Arroyo de Las Bandejas, ultimately reaching the southeast flowing Rio Bravo del Norte/ Rio Grande (Figure 1).

The sand comprising the SMD is predominantly quartz in composition, with estimates of 88 to 95 percent silica (Sanchez *et al.*, 2007; Dominguez Acosta, 2009), and the remainder being rock fragments (Webb, 1969; Sanchez *et al.*, 2007). The sands are rounded to well-rounded, well-sorted to very well-sorted, and predominantly fine-grained (Dominguez Acosta, 2009).

2. Methods

The area of the mobile dunes was measured in the QGIS Geographic Information System software (version 3.30). Geomorphological parameters (estimated dune height, crest-to-crest spacing and crest orientations) for the SMD were obtained with the use of Google Earth remote sensing data, and Digital Elevation Models (DEMs) available through Instituto Nacional de Estadística, Geografía e Informática (INEGI, 2022). These parameters are useful factors in creating dune atlases, classifying dune distributions within fields, and as a means of comparison between dunes of different fields (Lancaster, 1988; Ewing *et al.*, 2006; Zheng *et al.*, 2022). Using Google Earth georectified images and 5 m digital elevation data from INEGI (2022), the Google Earth and QGIS utilities were combined to map and measure the heights, spacings and orientations of dunes.

A map of relative dune heights was calculated using the local relief model from the Relief Visualization toolbox in QGIS (version 3.30) to create a local relief model covering the entire field for features with spacings of 1 to 100 m (Figure 2). The largest megastar dunes (see section 3.1.6)

are too large to accurately be measured using this method, but all of the smaller dune heights are accurately shown. The interdunes in the resulting map were 0 to -1.5 m below the mean elevation, with most of them at approximately -1 m. Dune elevations were estimated at 1 m greater than the modeled height, which matched observations made in the field.

Dune azimuths were calculated by creating a slope map from the DEM and classifying as lee faces areas with slopes greater than 18°. These areas were then converted to separate polygons. The azimuths of dune faces were estimated by using the centerline calculation in GRASS GIS software. Adjacent centerlines were merged using the dissolve command and then straightened. Dune spacing was calculated using the Relief

Visualization toolbox in QGIS (version 3.30) to create a local relief model covering the entire dune field for terrain spacings greater than 20 m. This resulted in a grid where each point is related positively or negatively to the cells around it. Dunes and interdunes were identified by visually comparing the hillshade model from the DEM to the values in the local relief model. Observation showed that local relief on dunes caused peaks within a dune to be resolved as separate features. Interdunes, however, were resolved as individual features.

Polygons were created from the grid model and all the dune features were deleted. Then, the centroid of each interdune was calculated. Finally, a distance matrix was calculated for the nearest four points to each interdune centroid and

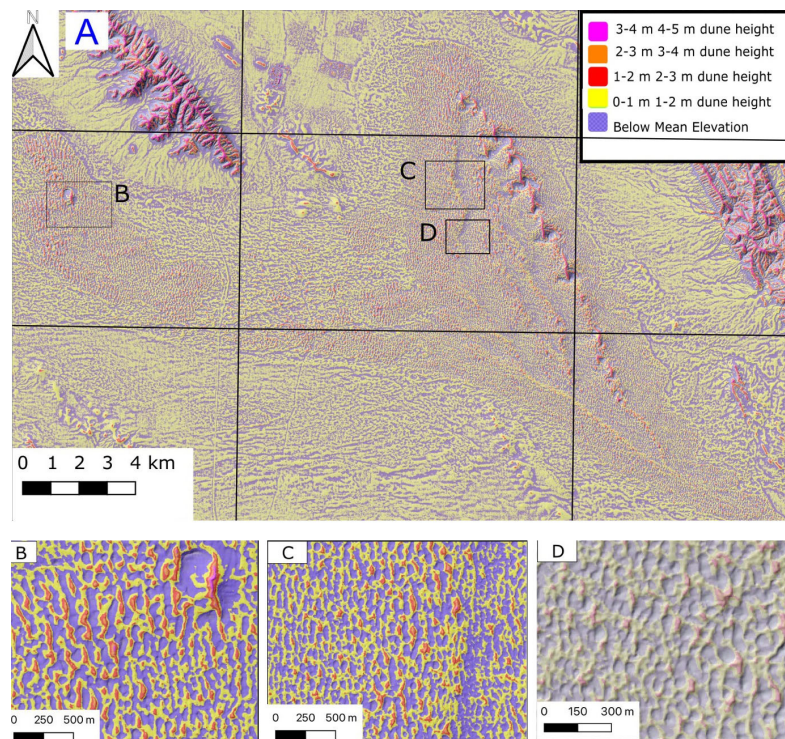


Figure 2 A) Map of relative dune heights created using the Multiscale Local Relief Model in the Relief Visualization Toolbox with distances between 1 and 100 m superimposed on a hillshade model of the 5-m resolution DEM from INEGI (2022). Note overall eastward increase in dune height, the increase in dune heights on the tops of the transverse ridges, and the fan shaped belts of larger dunes. B) Inset showing detail of the northwest field showing megastar dune and incipient star dunes (red and orange). C) Inset of the main dune field showing detail of interactions among the different smaller dune types. Taller star dunes show as red peaks. Note the increased dune heights on the relict transverse ridges. D) Inset showing smaller dune types in the topographical low between the western relict transverse dunes ridges.

contours were calculated from the resulting points (Figure 3). The model did not image the vegetated parabolic dunes, so the distances between apices of 100 adjacent dunes were measured in both along-wind, and across-wind directions. Centroids were calculated for each of the interdunes, a distance matrix was calculated, and the nearest four interdunes were averaged to provide a mean interdune spacing for each interdune.

Satellite data were confirmed by field measurements and the northern, western and

southern areas of the dunes were visited and sampled in the field. Walking a loop across the northern segment of the dune field, approximately 10 km long, led to the acquisition of topographical cross sections using a handheld GPS device. Data were analyzed by the device's GPS proprietary software. Six transects, four through the relict dune ridges and two across the megastar dunes, were measured to document dune height and spacing in the field.

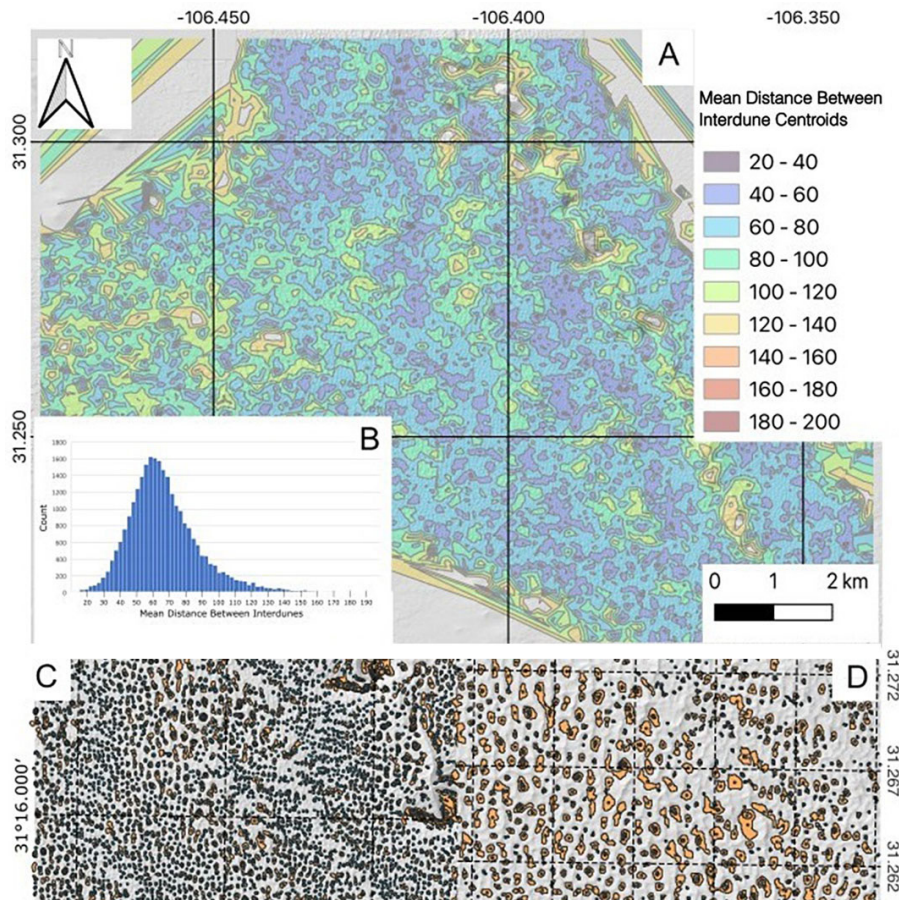


Figure 3 A) Map of interdune spacings from centroids of interdunes identified in local relief model in QGIS. Distances are the means of the four nearest interdune centroids to each point. Note that interdune spacings increase from west to east and dunes are more widely spaced on the tops of relict transverse ridges. B) Histogram of mean spacings for the 26,790 identified interdunes within the dune field. This includes interdunes between both north-south and east-west-trending dunes, average is 76.5 m and standard deviation is 23 m. The distance is calculated from the mean of the distances to the nearest 4 interdune centroids from the centroid of each interdune. C) Shows a representative sample of interdunes identified in the local relief model, superimposed on the shaded relief model from the 5 m resolution DEM (INEGI, 2022). D) Is a representative detail from the central dune field of the identified interdunes and hillshade map, showing the correspondence. The points are the centroids of the interdunes.

Table 1. Morphometric parameters of dunes in the SMD.

Dune Type	Average Length (m) (Across Wind for Parabolic)	Average Spacing or Range (m)	Average Height or Range (m)	Average Azimuth (degrees)
North-South Straight Crested Dunes	> 500	71	5	0.1°
East-West Straight Crested Dunes	66	91	5	96°
Vegetated Parabolic Dunes	88	150	Varies, degraded	Trend to ENE
Star Dunes	Irregular	Irregular	8-25	NA
Relict Transverse Dunes	4000-15000	800-1300	25-40	305°-335°
Very Large Star Dunes	~400-1400	384-2594	60-138	NA

3. Results

3.1 MORPHOMETRY AND DUNE FORMS

The SMD is shown to cover a total area of 139.7 km², separated into two bodies of sand ranging approximately 24 km long and 15 km wide for the main body covering an area of 113.8 km², and 9 km long by 6.5 km wide for the second body to the west and northwest, with an approximate area of 25.9 km².

The SMD exhibit a complex interrelation of at least six different dune forms (Table 1). These are north to south straight-crested dunes, east to west straight-crested dunes, vegetated parabolic dunes, star dunes, relict large transverse dunes, and very large star dunes (megastar dunes or draas) (Figures 4, 5). Sets of perpendicular, straight-crested dune patterns dominate the field surface (Figures 2, 5, 6). These dune patterns display a dominant north-south oriented dune set interlaced by a secondary and shorter east-west oriented dune set (Figures 2, 6). Totals of 19,957 north-south trending dune faces and 19,151 east-west trending dune faces were identified. Scattered throughout the field where the straight-crested dune patterns coalesce in an “aligned” position, a four to five-armed active star dune pattern emerges (dark red dunes

in Figure 2, Figure 5C). The eastern area of the field is dominated by the tallest of all dune forms in the SMD, a NNW-trending chain of multi-arm megastar dunes rising over 120 m from the surrounding interdune areas (Figures 1, 5A, 7). A total of 26,790 interdunes were identified in the SMD (Figure 3).

3.1.1 NORTH TO SOUTH STRAIGHT-CRESTED DUNES

The north to south straight-crested dunes form the most common and widespread dune form in the SMD (Figures 2, 4, 5D, 6). Although similar numbers of north to south and east to west trending dunes were identified, the greater length and continuity results in a more common distribution of north to south forms. These straight-crested dunes reach heights of approximately 5-7 m above the surrounding interdune areas and vary in length across the field. They display a clear and sharp crest, oriented north-south with a well-defined lee side, commonly facing east. The longest continuous dunes occur primarily in the northern segment of the main body of dunes, reaching up to 1.5 km long. Dunes in the eastern and southern segments of the main field may be as short as ~160 m, but the average dune length is over 500 m. The north to south trending dunes become taller and more widely spaced as they pass over large relict

transverse dunes, reaching maximum heights on the crests (Figures 2, 6). Dune defects in the forms of tuning-fork junctions are common in the field, representing normal dune response to variations in the wind patterns (Beveridge *et al.*, 2006) and varying migration rates (Ewing *et al.*, 2006; Ewing and Kocurek, 2010b). The crest-to-crest spacing averaged 71.1 m with a minimum spacing of 20 m, a maximum spacing of 124 m and a standard deviation of 20 m (Figure 6).

These and the east to west straight-crested dunes (Figure 2, 5B, 7) are active and superimposed atop the relict transverse dunes, with which they form compound and complex dune relations (Kocurek *et al.*, 2005; Beveridge *et al.*, 2006; Ewing *et al.*, 2006). Maps of dune heights and spacings show trends on a variety of scales (Figures 2 and 6). There is an overall increase in both dune heights and spacings from west to east, downwind across

the SMD coinciding with an overall increase in dune size (Figures 2, 6). Superimposed on this are increases in heights and spacings toward the crests of the relict transverse dunes (Figures 2, 3).

3.1.2 EAST TO WEST STRAIGHT-CRESTED DUNES

The east to west straight-crested dunes are oriented transverse to the secondary local wind regimes from the north and south (Figures 1, 6). A distinct characteristic of these dunes is the lack of well-defined, sharp crests in response to varying winds (Figure 5D, 5E (background), 5F). This is exemplified by the presence of rounded dune tops with the absence of brink and avalanche faces. Steeper faces are more common on the North sides of east to west trending crests (Figure 2B). Similarly to the conjugate north to south dunes, the east to west dunes reach heights up to approximately 5 m from their interdune areas (Figures 2, 7).

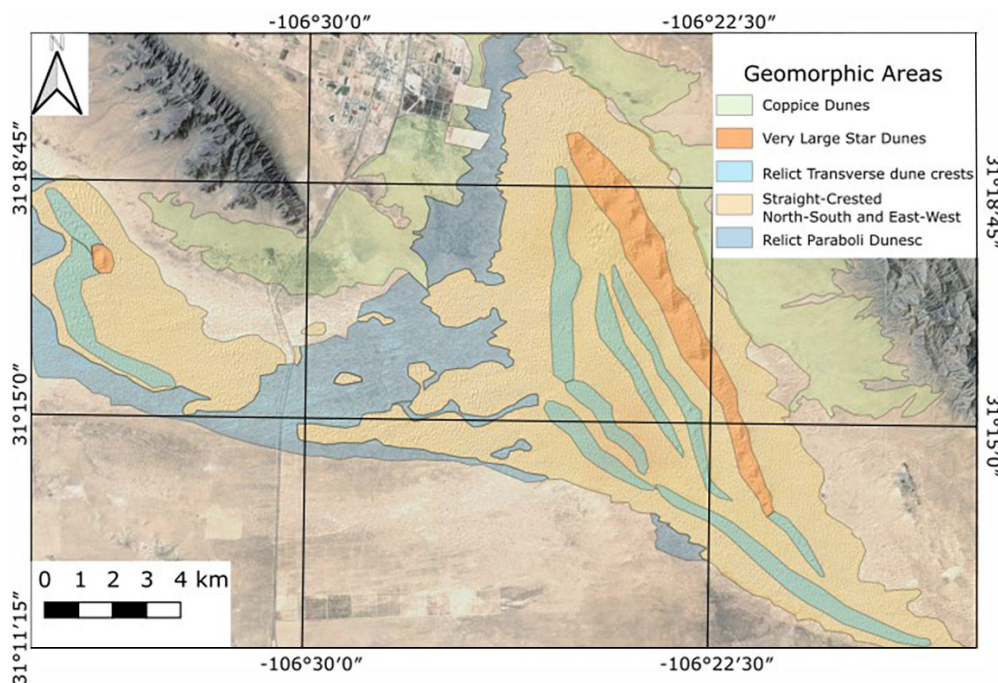


Figure 4 Geomorphic map showing the distributions of different dune morphologies in the SMD field. Coppice dunes flank the field to the east, north and south, but lie outside of the dune field proper. Vegetated parabolic dunes are found in parts of the dune field not covered with active dunes and generally define a surface that underlies the active dunes. Relict transverse dunes are evident as large features with steep northeastern faces that the active straight crested dunes cross at angles. A chain of megastar dunes forms the eastern and most prominent ridge line, complexly juxtaposed on top of the easternmost relict transverse dune. An isolated megastar dune is located in the smaller upwind dune field. Simple star dunes (not shown) are scattered within the zone of straight crested dunes.

The length of these dunes varies across the field where the longest dunes reach lengths of ~225 m while the smaller ones are approximately 50 m. The average length of these dunes is 66 m, the maximum lengths for these dunes are reached when two or more east-west crests intersect across one or more north-south dunes, giving the appearance of a single and extended dune crest generally aligned east to west.

3.1.3 VEGETATED PARABOLIC DUNES

The straight-crested dunes are burying older vegetated dunes with degraded parabolic geometries (Figures 4, 8). Within the relict vegetated areas, northeast-trending mounds are the most common feature. These commonly terminate into hairpin bends into northwest-trending mounds. The steepest sides are on the outer flanks of these features, suggesting parabolic

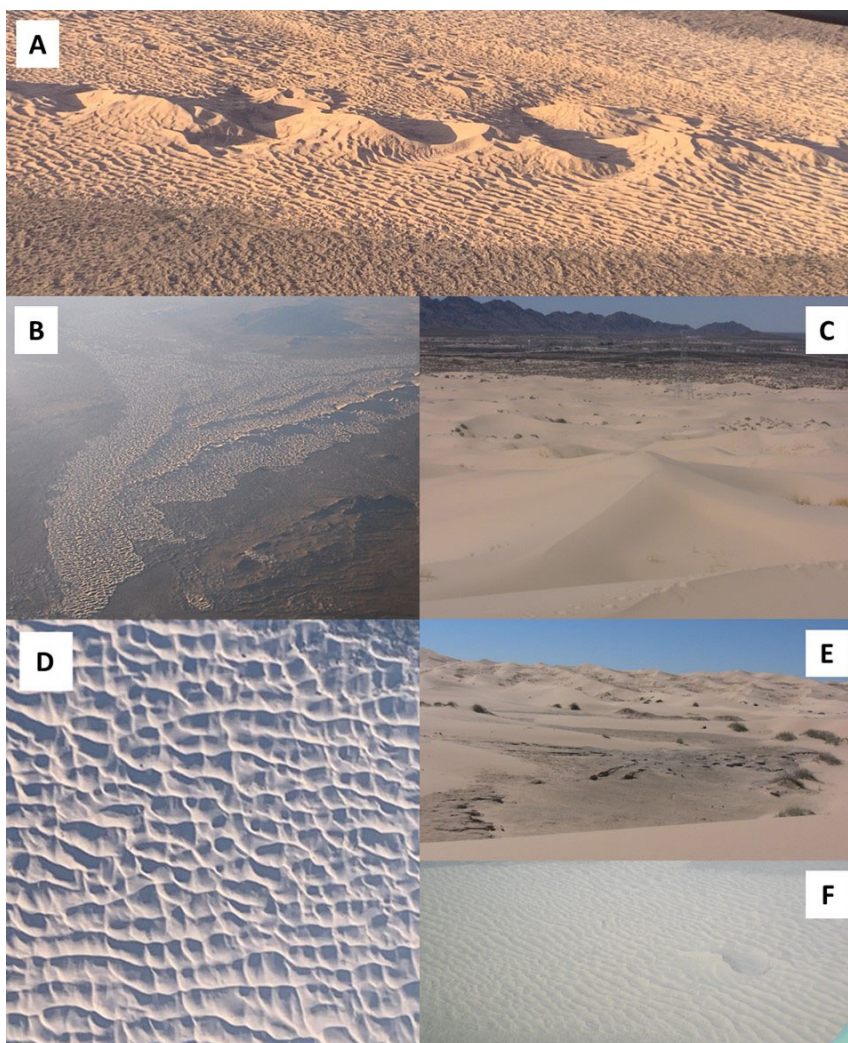


Figure 5 Photos of dunes in the Samalayuca dune field. A). Very large star dunes (Megastar dunes) (Draas) in the northern segment of the main dune field, flanked by straight crested north to south dunes and a noticeable relic transverse ridge west of the megastar ridge. View to the W; B). Main dune field, view to the N-NW. Eastern ridge is the megastar dunes, west of it the relic transverse ridges are noticeable; C). Simple star dune (center of figure), formed by the compound interaction of north-to-south and east-to-west crested dunes. View to the west. D). Straight-crested dune sets, north to south are more prominent with longer crests than the east to west set. Southeast area of the SMD; E). North to south straight-crested dunes in the northern section of the main field. Interdune area with consolidated cross-strata in the foreground. View to the south; F). Western dune field (smaller), prominent ridges are the north to south straight-crested dunes. Larger ridge is an isolated megastar dune. View to the SW.

origin. The relict vegetated parabolic dunes have more gentle slopes, and therefore are indicated as areas of widely spaced dunes without identified dune faces in Figure 6.

The vegetation on the dunes varies due to grazing and other human disturbance as well as variation in precipitation. However, in general, the vegetated dunes are one of the most productive parts of the landscape due to the ability of the sand to retain precipitation (Gobierno del Estado de Chihuahua, 2023). Vegetated and partially stabilized areas are dominated by mesquite (*Prosopis juliflora*), chamiso (*Atriplex canescens*), and sand sagebrush/estafiate (*Artemisia filifolia*). Grass

species common in the dunes include black grama (*Bouteloua eriopoda*), blue grama (*Bouteloua gracilis*), and alkali sacaton (*Sporobolus airoides*).

3.1.4 STAR DUNES

Star dunes of different sizes are scattered across the field (Figures 2, 5C). Some of the smaller and incipient star dunes possess a four-arm morphology generated by the onset intersection of east to west and north to south straight-crested dunes (Figures 2, 5C). As these intersecting patterns accumulate more sediments, the center area (star vertex) continues growing, developing a sharp peak and giving rise to an incipient four- or five-armed

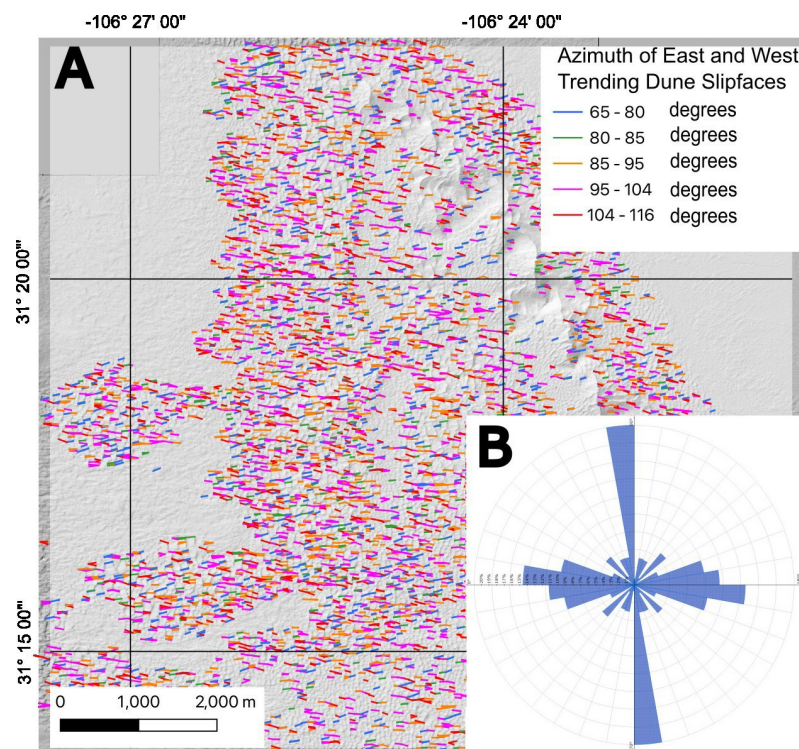


Figure 6 A) Map of dune orientation in central part of the SMD. Lines represent slip faces of dunes identified using slope and aspect maps from the 5m DEM from INEGI (2022). Colors denote the azimuths of east-to-west dune trends. Note the longer southeast-trending dunes and the rotation of dune crests toward the southeast on the eastern sides of larger forms. B) Rose diagram showing the distribution of dune face azimuths from the 39,108 identified dune faces. Note the predominant north-south trend and greater spread in the east-west trends.

star dune (Werner, 1995). The larger star dunes commonly are seated on and are reworking the relict transverse dunes. Star dunes increase in size, frequency and complexity towards the east, as they position atop higher areas of the relict transverse dunes (Figures 2, 7). These star dunes may exhibit four to six arms, commonly formed by a north-south crest intersected by one or more east-west crests and/or oblique versions of the same east-west crests, and reach lengths up to approximately 300 m (Figure 5C).

3.1.5 RELICT TRANSVERSE DUNES

The SMD displays a set of six large transverse dune ridges underlying all other dune types in the field except for the vegetated parabolic dunes (Figures 2, 4, 7). Five of these ridges are in the main dune field. The three southeastern ridges extend across the field almost parallel to the northeastern, downwind field margin, striking NNW to SSE and transverse to the westerly/southwesterly prevailing winds (Figures 4, 7). These ridges display an average ridge-to-ridge spacing of ~1

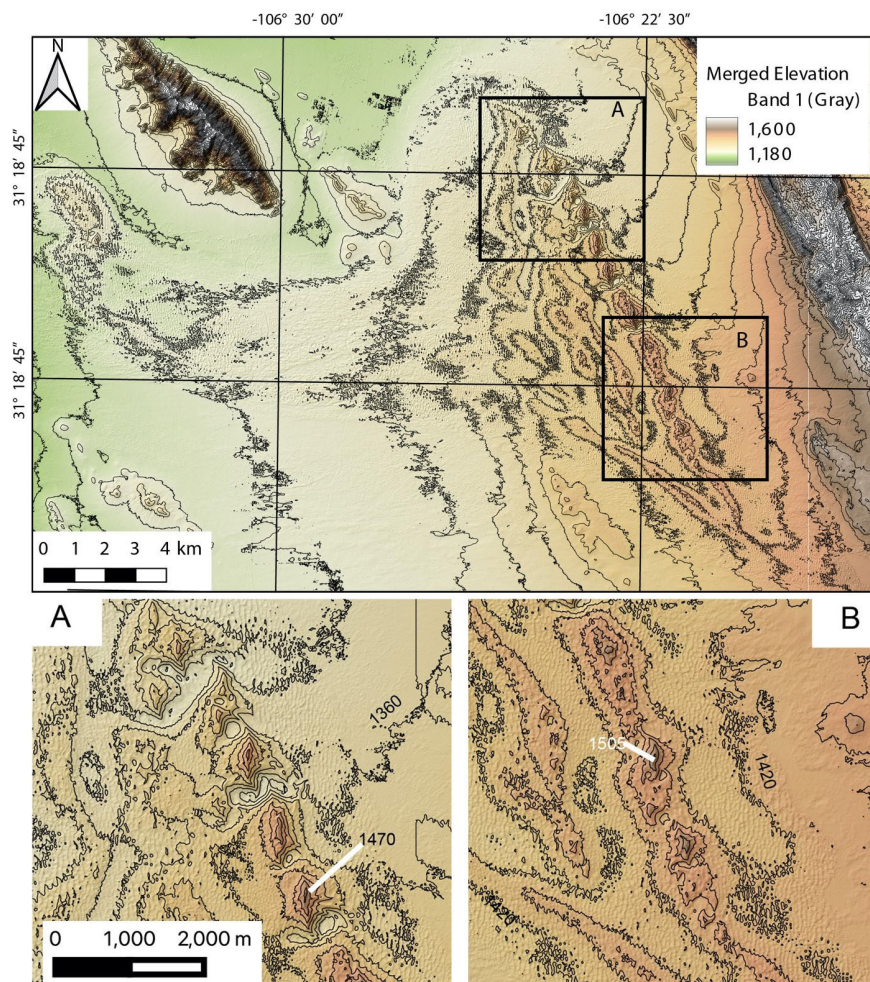


Figure 7 Shaded topographic map of the Samalayuca dune field. The north-northwest-trending relict transverse ridges are visible as 1 km-wide topographic highs 25 to 40 m above the adjacent troughs. These ridges form the underlying skeleton of the SMD field and represent the older preserved dune features. The megastar dunes are evident on the northeasternmost ridge of the dune field. A) Detail of northern megastar dunes, note the northeast-trending depressions on the south sides of the dunes. The north-south-trending dunes are deflected toward the megastar dune and assume a northeast trend. B) Detail of the southern megastar dunes, note the more continuous ridge underlying them and the *en-echelon* offset of the crests. Deflection of the north-south-trending crests does not extend as far from the megastar dunes. Contour interval is 20 m. Data is from 5m resolution DEMs from INEGI (2022).

km and height of 40 to 50 m, with the inter-ridge areas occupied by troughs. The southwesternmost ridge extends 3 km southeast of the easternmost ridge, on which the megastar dunes have formed and which terminates against this ridge. It extends northwest, trending at 307°, and becomes the westernmost ridge, except for a more subdued vegetated ridge 1.5 km to the southwest. Another shorter transverse dune ridge trends northwest at an angle between the eastern ridges and the southern ridge with an azimuth of 315°, filling the remaining angle between the long southern ridge and the three eastern ridges (Figures 4, 7).

The transverse ridges rise and fall along their length, gradually becoming wider and taller and then shorter and narrower, with wavelengths of 1.5 to 3 km (Figure 7). They are also asymmetrical with steeper western flanks and more gentle eastern flanks. This is most evident on the map of dune heights (Figure 2).

The northwest body of dunes against the Sierra de Samalayuca exhibits a single similar ridge located at the upwindmost part of the field and extending for almost 6 km in a general NNW direction, forming an upright Z shape (or

“lightning bolt” shape). Similar to the main body of dunes, this ridge forms the highest topographical point in the northwest dune field (Figures 2, 4).

3.1.6 MEGASTAR DUNES

In the SMD field, a north-northwest oriented chain formed by at least 15 multi-arm megastar dunes dominates the desert landscape, forming the tallest dune forms (Figures 4, 5A, 7). The megastar dunes follow the same alignment in an *en-echelon* pattern, with each dune offset 250-500 m to the northwest/southeast of adjacent dunes (Figures 5A, 5B). Each megastar has the same general form, a north-south-trending ridge that rises to a peak, while oblique east-west-trending arms descend the flanks. On the western (upwind) lower flanks of the larger northern dunes, the arms curve to the south and merge into the smaller north-south trending straight-crested dunes near the base (Figures 5A, 5B). On the eastern (downwind) flanks and on both sides of the smaller southern dunes, the arms curve to the north and form an interference pattern with the north-south trending dunes. The north-south trending dunes are deflected toward the megastar dunes as they approach the bases (Figures 7A, 7B).

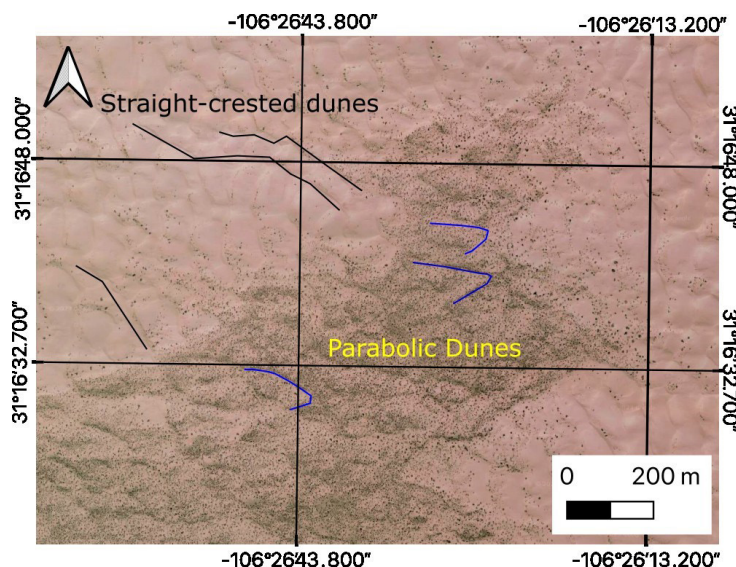


Figure 8 Older vegetated parabolic dunes being covered by younger straight-crested dunes. Image from PlanetScope, April 28, 2023. Black lines trace the crest of some of the straight-crested dunes. Blue lines trace the crests of some of the vegetated parabolic dunes. Parabolic dunes show the characteristic sharply curved apex pointing downwind.

Each of the megastar dunes is flanked by east-west elongate depressions on their south sides. These are deeper in the north, where they extend as much as 80 m below the average surface (Figures 5A, 5B). These scours are flanked with consolidated aeolian sands that also expose thin limestone, possibly of lacustrine origin. The topography and exposed materials imply deflation south of the megastar dunes. This is likely due to the deflection of wind around the dunes, forming vortices, although it is not clear why this is concentrated at the south ends of the dunes. The erosional depressions become smaller and shallower to the south along the chain of megastar dunes (Figure 5B).

Added to this complexity, small climbing dunes are superimposed on the upwind (SE) sides of the megastar dunes as a likely result of vortex winds generated by the topographical barrier (Figures 5A, 5B). The straight-crested dune sets form climbing dunes atop the megastar dunes (draas) of the easternmost dune ridge (Figure 7), forming a complex relationship with them due to the effects of the very large star dunes on local wind patterns. On the star dunes, the east-west dune orientations are deflected toward a more northwest crest trend (Figure 7). Similarly, the north-south-trending dunes are deflected from their original north-south patterns to north-northeast on the upwind side of the larger structures and north-northwest on the downwind side of the underlying dunes. The average crest-to-crest spacing also increases as both sets of dunes interact more closely with the larger forms (Figure 3).

3.1.7 INTERDUNES

Interdune areas formed by the intersecting patterns of the dominant north to south and east to west straight-crested dunes are another characteristic feature of the SMD. They form bowl-shaped deep hollows widespread across the entire field creating the appearance of square honeycomb patterns (Figures 2, 3, 5E). The local relief model identified a total of 26,790 interdunes (Figure 3). Areas of larger dune spacings correlate with the star dunes, with the largest spacings on the megastar dunes.

Greater spacings are also found on the crests of the relict transverse dunes (Figures 2, 3, 7), while the areas with the smallest spacings are found in the lees of the relict transverse dunes (Figures 3, 7).

4. Discussion and conclusions

Analysis of the morphometry of a dune field, such as the SMD, can shed light on the dune field's history, activity, formation, and stability, and especially its response to the local environmental parameters and their changes through time. Morphometric measurements are also useful to contextualize and compare a dune field's component dune dimensions to those of others worldwide (Table 2).

In the context of the main descriptive parameters of global sand seas (Lancaster, 2022), the SMD is a small erg, a (presently) dry aeolian system representing multiple generations and forms of dunes composed of mineralogically mature quartz. As with the White Sands to the north (McKee, 1966; Fryberger, 2001; Langford, 2003; Kocurek *et al.*, 2007; Langford *et al.*, 2009), its sediment supply originates from a playa system. Its orientation and geometry appears to be topographically controlled by sand accumulation upwind of topographic highs (in the case of the SMD, the Sierra del Presidio and Sierra de Samalayuca), where wind velocity is checked at the base of a mountain mass and local wind regimes give rise to star and other complex dune forms (Lancaster, 2022), similar to the Great Sand Dunes in Colorado, USA (Valdez and Zimbelman, 2020). The wind regime associated with the formation of the SMD is characterized by winds from multiple directions with changing seasons, leading to development of star dunes and megastar dunes, as is also seen in the Gran Desierto sand sea in Sonora, Mexico (Beveridge *et al.*, 2006; Lancaster, 2022).

Table 2. Morphometric parameters of main dune types in representative locations (Lancaster, 1995) and morphometric parameters of main dune types in the SMD in italics. Range in parentheses.

<i>Dune type / Location</i>	<i>Spacing (m)</i>	<i>Width (m)</i>	<i>Height (m)</i>
Simple crescentic / Straight crested			
White Sands	112 (60 – 198)	72 (30 – 185)	
United Arab Emirates	590 (70 – 2000)	440 (100 – 1100)	
AlJiwa	630 (200 – 1000)	590 (200 – 900)	
Thar Desert	580 (200 – 1000)	470 (500 – 1500)	
Takla Makan	590 (500 – 1200)	630 (200 – 1000)	
Namib Sand Sea	272 (100 – 400)		8.25 (3 – 10)
Skeleton Coast	259 (90 – 645)	21 (4 – 56)	
Gran Desierto	150 – 400 (sic)		
<i>Samalayuca</i>	<i>71.1 (20 – 124) N-S</i> <i>91 (16-135) E-W</i>		<i>5 - 7 N-S; ~5 E-W</i>
Compound crescentic / Relict transverse			
Nafud	1840 (800 – 3300)	800 (500 – 2000)	
Rub 'al Khali	1430 (850 – 2200)	670 (300 – 1100)	
Thar Desert	1440 (700 – 2500)	1300 (750 – 2000)	
Takla Makan	3000 (2000 – 5000)	2200 (1100 – 3400)	
Aoukar	1710 (1000 – 2500)	1590 (1200 – 2100)	
NW Sahara	650 (300 – 1500)	1240 (500 – 2000)	
Namib	694 (800 – 1200)	680 (300 – 1200)	18.6 (10 – 40)
Algodones	1070 (400 – 2500)	880 (500 – 2500)	50 - 80 (sic)
Gran Desierto	1380 (500 – 2300)	660 (300 – 1500)	20 - 100 (sic)
<i>Samalayuca</i>	<i>~1000 (800- 1300)</i>	<i>780 (700-1,100)</i>	<i>25 - 40</i>
Star / Megastar			
Namib	1330 (600 – 2600)	1100 (400 – 1000)	145 (80 – 350)
Niger	1000 (150 – 3000)	610 (200 – 1200)	
Grand Erg Oriental	2070 (800 – 6700)	950 (400 – 3000)	117
SE Rub' al Khali	2060 (970 – 2860)	840 (500 – 1300)	(50 - 150) (sic)
Ala Shan	137 (300 – 3200)	740 (400 – 1000)	(200 – 300) (sic)
Gran Desierto	2982 (1500 – 4000)	2092 (700 – 6000)	
<i>Samalayuca</i>	<i>1179 (384 – 2594)</i>	<i>840 (400- 1400)</i>	<i>98 (60 - 138)</i>

4.1 ANALYSIS OF SAMALAYUCA DUNE FORMS

The SMD is shown to cover a total area of ~139.7 km², separated into a main body covering an area of 113.8 km², and a second body to the west and northwest with an area of 25.9 km². The SMD exhibit six major dune forms (Table 1 and Figure

4) that are likely created and maintained by interactions between the surrounding mountains and a complex wind regime. Compound dunes form when a specific type of dune interacts with similar types to create a larger dune. Complex dunes form through interaction of different dune forms. These relations are exemplified when a

dune form is overlaid by different dune forms both geomorphically and chronologically (Lancaster, 1995; Kocurek *et al.*, 2005; Ewing *et al.*, 2006). The Samalayuca dunes contain both compound and complex dune forms, as is typical in global dune fields and sand seas (Barchyn and Hugenholtz, 2015; Lancaster, 2022). Table 2 compares some of the morphometric characteristics of key dune types within the SMD to similar features in other sand seas.

The east to west and north to south straight-crested dunes are the most mobile and widespread dune forms in the SMD. The north-south oriented dunes resemble “crescentic ridges” (Lancaster, 1995) or “transverse ridges” (McKee, 1979). However, they are oblique to the prevailing winds, and therefore we have not used the term transverse dunes. They are common throughout the world’s sand seas and constitute the dominant form in several large-scale dune fields such as the Thar Desert, the Takla Makan, and Tengger sand seas (in Asia); and the Jafurah, Nafud and parts of the Rub’ al Khali (in Saudi Arabia and the northern Sahara Desert) (Fryberger and Goudie, 1981). In North America, transverse/crescentic ridged dunes range from very widespread to common in most sand seas (Lancaster, 1995) including those in the Chihuahuan Desert (White Sands; Ewing and Kocurek, 2010b, and here at the SMD). In the SMD, these dunes are active, comprise the most mobile features in the field, and represent a response to seasonal changes in wind directions and atmospheric conditions. The orientation of these “transverse ridge” or “crescentic ridge” dunes and their crests are a response to the local prevailing westerly winds (Schmidt and Marston, 1981). The Samalayuca dunes differ from the typical transverse dunes in that they are oblique to the prevailing wind in the region and interact with similarly sized dunes at right angles, an almost unique pattern in the world.

The large transverse dune ridges that form the large-scale framework of the main field reach as high as 40 m, not including the height of the star and megastar dunes that crown them. Due to their

gentle lee slopes and discordance with the trends of the active dunes, the transverse ridges are interpreted as relict forms. Because the southern ridges are vegetated, these ridges are interpreted to have formed in an earlier episode of aeolian activity, preceding the current (likely Holocene) event (Figures 5B, 7). A similar scenario is present in some other large and old dune fields, where relict linear dunes underlie younger superimposed dune forms, such as the Gran Desierto sand sea in Sonora (Kocurek and Ewing, 2005; Beveridge *et al.*, 2006). The spacing and height of these relict transverse dunes at the SMD are within the range of similar features in other global dune fields (Table 2)

Vegetated parabolic dunes underlie the active dunes at the SMD. Vegetated and active parabolic dunes are common, both in the region and around the world in vegetated aeolian landscapes (Goudie, 2011), including the White Sands dune field to the north (Fryberger, 2001; Langford, 2003). Parabolic dunes vary in size, both locally and from field to field, in part due to differences in sand supply, climate, and local geomorphic factors (Hugenholtz *et al.*, 2008; Nield and Baas, 2008; Langford *et al.*, 2009). Vegetated parabolic dunes strongly resemble other parabolic dunes and form within the expansive size range of parabolic dunes (Goudie, 2011).

We should note that while we differentiate the star dunes and megastar dunes at the SMD, other authors have included all of these together, as the fields they describe have a greater and more continuous size range (Lancaster, 1989; Goudie *et al.*, 2021). Around the world’s dune fields, megastar dunes form less than 10% of the dune forms in sand seas that contain them, commonly forming the highest dune forms in these areas (Lancaster, 1995; Goudie *et al.*, 2021). Star dunes, including large star dunes, have been described in other ergs in Africa, Saudi Arabia, China and North America (McKee *et al.*, 1974; Bishop, 2013; Dong *et al.*, 2004; Goudie and Viles, 2015; Goudie *et al.*, 2021) (Table 2). In North America descriptions of such dunes have been made for the

Gran Desierto, Kelso, Dumont and Eureka dune fields (Sharp, 1966; Lancaster, 1995; Beveridge *et al.*, 2006, Goudie *et al.*, 2021).

The heights and spacings of star dunes at the SMD fall within the size range of smaller dunes described in the Gran Desierto of Sonora (Lancaster, 1989; Lancaster and Hesp, 2020). The largest SMD star dune forms lie at the upper limit of heights and spacings in the Gran Desierto (Lancaster, 1989), and smaller star dunes in the Gran Desierto also form on transverse ridges of sand as at the SMD (Lancaster, 1989). Similarly, the heights and spacings of the SMD star dunes fall well within the size ranges of star dunes described from elsewhere on Earth (Goudie *et al.*, 2021) (Table 2). The Samalayuca dunes fall into the Type 9 of Goudie *et al.* (2021), where star dunes form on a transverse dune.

What differentiates the SMD's star dunes from most of those elsewhere is their evident interactions with the straight-crested dunes in the field. Many dune fields exhibit star dunes that are isolated from each other by sand sheets or other low-relief features (Lancaster, 1989; Goudie *et al.*, 2021). While individually complex, their relationships with flanking features are obscure. However, most of the arms of the SMD star dunes extend away from the star and continue as east to west trending or north to south trending straight-crested dunes (Figures 2, 5A). Also, as the star dunes at the SMD increase in size, the straight-crested dunes are deflected inward, toward the peak of the dune (Figure 7). Therefore, while the SMD star dunes are representative of star dunes around the world, they provide rare examples of the interactions between star dunes and other dune types due to the deflection of smaller dunes on their flanks. A more detailed analysis of these features in the future, for example modeling of how increasing dune size changes wind flow around the dunes, would provide important information about similar dunes across the solar system.

The SMD's star and megastar dunes may form by the ongoing accumulation of sand derived from the interaction of multiple wind directions

caused by the coalescence of the prevailing local westerly winds in conjunction with localized eddy-like currents generated at the upwind base of the megastar dunes. Added to these wind currents are the presence of localized "backward" northeasterly winds generated by the shadow effect of the Sierra del Presidio and the secondary opposing local wind directions both from the north and south.

4.2 PAST AND FUTURE OF THE SAMALAYUCA DUNES

The SMD sand sea is the largest active, non-nabkha dune field in the Chihuahuan Desert of México. The Samalayuca Dunes were first mentioned over 400 years ago, by Spanish colonizers who first ventured through the region as they traveled north (Schmidt and Marston, 1981). The dunes represented a significant obstacle to expedition parties traveling along the *Ruta de Oñate* portion of the *Camino Real de Tierra Adentro* (Sanchez, 2017) between México City and Santa Fe. Nowadays, motorists speed by the dunes on México Federal Highway 45 between Ciudad Juárez and Chihuahua city. The dunes are currently a popular tourism area for hiking, photography, sandboarding, and some off-road vehicle use. Off-road vehicle activities have been taking place in the sands for at least 55 years (Vázquez Bernal, 2022). The SMD have even been used as a cinematic setting for an alien world, in David Lynch's film "Dune" (Lorenz and Zimelman, 2014).

The dune field has been protected since 2009 within the *Área de Protección de Flora y Fauna Médanos de Samalayuca* (Gobierno del Estado de Chihuahua, 2023), which covers 63,182 hectares. The dune field has also been the subject of some past proposals for extractive use. Sanchez *et al.* (2007) found the sands suitable for exploitation for glass, stating "the detailed study from Samalayuca sand dunes show a possible perspective for the development of an exploitation project and the sand can be used in manufacture of flat glass and as raw materials in glass and ceramics industries."

Because of the number of potential commercial and recreational uses of the SMD,

better understanding the processes that shape and maintain these dunes is critical. This initial research on the SMD's morphometry has laid down a basic understanding of the current state of the sand sea and the dune forms that comprise it. Understanding the controls on sand supply, the geological history and dynamics of the sand sea, and the interplay of different dune types may aid especially in maintaining the megastar dunes that are the most unique and dramatic features in the field. As a protected area, the SMD's management and conservation requires a detailed knowledge of its physical workings, including its morphometry, which can help guide designation of areas more suitable for various recreational activities versus those areas which may need to be preserved with as little disturbance as possible, and also suggest how different sections of the dune field may respond to regional land cover and climatic change.

Much more geological research remains to be done on the SMD, and many scientific questions remain about this sand sea. When did the SMD first form? What is the total volume of sand in the SMD? How have the morphometry of the sand sea, the dynamics of its dune forms, and its sand sources changed over time, from recent decades to the Pleistocene? What was the state of the ancestral dune field when the now-relict transverse dunes were active and perhaps the dominant dune form? What are the individual dune types movement rates? How has sediment supply to the SMD changed over time? How much sand is being added to, or lost, from the SMD under the current climate, and how will it change with projected climate change scenarios? Exactly how do Sierra del Presidio and Sierra Samalayuca and other topographic obstacles control the dynamics of the SMD?

These and other scientific questions have a profound implication regarding any management plan for a remarkable geologic monument such as the SMD. As a geological and natural showpiece of Chihuahua and México, the Samalayuca Dunes (Médanos de Samalayuca) should be maintained as a protected area and sustainably managed.

Contributions of authors

(1) Conceptualization: MDA, RPL, TEG (2) Analysis: MDA, RPL (3) Methodologic/technical development: MDA, RPL, TEG (4) Writing of the original manuscript: MDA (5) Writing of the corrected and edited manuscript: TEG, RPL, MDA (6) Graphic design: MDA, RPL (7) Fieldwork: MDA, RPL (8) Interpretation: MDA, RPL, TEG

Financing

The study was done without financial sponsorship.

Acknowledgements

We acknowledge the help and participation of late Dr. Robert H. Schmidt Jr, whose article "Geomorphologic Parameters of Los Médanos de Samalayuca, Chihuahua", set the initial scenario for the SMD chapter in the Ph.D. dissertation that gave rise to this manuscript (Dominguez Acosta, 2009). We also acknowledge the help of Sergio Alvarado Soto M.S. from Universidad Autónoma de Ciudad Juárez in the preparation of some of the location images for the SMD.

Conflicts of interest

The authors identify no conflict of interest.

References

- Baddock, M.C., Gill, T.E., Bullard, J.E., Dominguez Acosta, M., Rivera Rivera, N.I., 2011, Geomorphology of the Chihuahuan Desert based on potential dust emissions: *Journal of Maps*, 7(1), 249-259. <https://doi.org/10.4113/jom.2011.1178>
- Barchyn, T.E., Hugenholtz, C.H., 2015, Predictability of dune activity in real dune fields under unidirectional wind regimes: *Journal of Geophysical Research- Earth Surface*, 120, 159- 182. <https://doi.org/10.1002/2014JF003444>

- org/10.1002/2014JF003248
- Beveridge, C., Kocurek, G., Ewing, R.C., Lancaster, N., Morthekai, P., Singhvi, A.K., Mahan, S.A., 2006, Development of spatially diverse and complex dune-field patterns: Gran Desierto Dune Field, Sonora, Mexico: *Sedimentology*, 53(6), 1391 – 1409. <https://doi.org/10.1111/j.1365-3091.2006.00814.x>
- Bishop, M.A., 2013, Dune field development, interactions and boundary conditions for crescentic and stellate megadunes of the Al Liwa Basin, the Empty Quarter: *Earth Surface Processes and Landforms*, 38(2), 183-191. <https://doi.org/10.1002/esp.3318>
- Cervantes-Rendón, E., Ibarra-Bahena, J., Cervera-Gómez, L.E., Romero, R.J., Cerezo, J., Rodríguez-Martínez, A., Dehesa-Carrasco, U., 2022, Rural application of a low-pressure reverse osmosis desalination system powered by solar-photovoltaic energy for mexican arid zones: *Sustainability*, 14(7), 10958. <https://doi.org/10.3390/su141710958>
- Dominguez Acosta, M., 2009, The Pluvial Lake Palomas- Samalayuca Dune system. El Paso, USA, University of Texas at El Paso, Ph.D. dissertation. p. 261.
- Dominguez Acosta, M., Gill, T.E., 2007, PIXE based geochemical characterization of the Pluvial Lake Palomas - Samalayuca Dunes corridor system, Chihuahua, Mexico, in *Proceedings, XI International Conference on Particle Induced X-Ray Emission and Its Analytical Applications*, Puebla, Mexico, PII-33.
- Dominguez Acosta, M., Gill, T.E., Schmidt, R.H. Jr., 2006, The Lake Palomas – Samalayuca Dune corridor system, Chihuahua, Mexico (abstract), in *Sixth International Conference on Aeolian Research*, Guelph, Ontario, Canada, p. 80.
- Dong, Z., Wang, T., Wang, X., 2004, Geomorphology of the megadunes in the Badain Jaran Desert: *Geomorphology*, 60(1-2), 191-203. <https://doi.org/10.1016/j.geomorph.2003.07.023>
- Enriquez Anchondo, I.D., 2003, Las cactáceas de Samalayuca: Ciencia en la frontera: revista de ciencia y tecnología de la UACJ, 2(1), 55- 62.
- Ewing, R.C., 2020, White Sands, in: Lancaster, N., and Hesp, P. (Eds.), *Inland Dunes of North America*: Springer, Cham, 207- 237. https://doi.org/10.1007/978-3-030-40498-7_6
- Ewing, R.C., Kocurek, G.A., 2010a, Aeolian dune-field pattern boundary conditions: *Geomorphology*, 114 (3), 175–187. <https://doi.org/10.1016/j.geomorph.2009.06.015>
- Ewing, R.C., Kocurek, G.A., 2010b, Aeolian dune interactions and dune-field pattern formation: White Sands Dune Field, New Mexico: *Sedimentology*, 57(5), 1199-1219. <https://doi.org/10.1111/j.1365-3091.2009.01143.x>
- Ewing, R.C., Kocurek, G.A., Lake, L.W., 2006, Pattern analysis of dune-field parameters: *Earth Surface Processes and Landforms*, 31(9), 1176 – 1191. <https://doi.org/10.1002/esp.1312>
- Fryberger, S.G., 2001, Geological overview of White Sands National Monument.
- Fryberger, S.G., Goudie, A.S., 1981, Arid geomorphology: *Progress in Physical Geography: Earth and Environment*, 5(3), 420 – 428. <https://doi.org/10.1177/030913338100500305>
- García-DelaPeña, C., Gadsden, H., Palomo-Ramos, R., Gatica-Colima, A.B., Lavin-Murcio, P.A., Castañeda, G., 2012, Spatial segregation of microhabitats within a community of lizards in Médanos de Samalayuca, Chihuahua, Mexico: *The Southwestern Naturalist*, 57(4), 430-434. <http://dx.doi.org/10.1894/0038-4909-57.4.430>
- Gobierno del Estado de Chihuahua, Áreas Naturales Protegidas de Chihuahua. Secretaría de Desarrollo Urbano y Ecología. http://www.chihuahua.gob.mx/sedue/areas_protegidas_chih, Accessed 6 March 2023.
- Goudie, A.S., 2011, Parabolic Dunes: Distribution, Form, Morphology and Change: *Annals of*

- Arid Zone, 50(3-4), 1-7.
- Goudie, A.S., Goudie, A.M., Viles, H.A., 2021, The distribution and nature of star dunes: A global analysis: *Aeolian Research*, 50, 100685. <https://doi.org/10.1016/j.aeolia.2021.100685>
- Goudie, A.S., Viles, H., 2015, Sossus Vlei and its Star Dunes, in Goudie, A. and Viles, H. (Eds.), *Landforms and Landscapes of Namibia*. Springer, Cham, 129- 131. https://doi.org/10.1007/978-94-017-8020-9_19
- Hall, S.A., Goble, R.J., 2015, OSL age and stratigraphy of the Strauss sand sheet in New Mexico, USA: *Geomorphology*, 241, 42-54. <https://doi.org/10.1016/j.geomorph.2015.03.032>
- Hawley, J.W., Hibbs, B.J., Kennedy, J.F., Creel, B.J., Remmenga, M.D., Johnson, M., Lee, M.M., Dinterman, P., 2000, Trans-international boundary aquifers in southwestern New Mexico. New Mexico Water Resources Research Institute, Report X996350-01-03.
- Hugenholtz, C.H., Wolfe, S.A., Moorman, B.J., 2008, Effects of sand supply on the morphodynamics and stratigraphy of active parabolic dunes, Bigstick Sand Hills, southwestern Saskatchewan: *Canadian Journal of Earth Sciences*, 45(3), 321-335. <https://doi.org/10.1139/E08-001>
- Instituto Nacional de Estadística, Geografía e Informática (INEGI), 1983, Carta Geológica (Geological Map), Ciudad Juárez, 1:250,000, Hoja (Sheet) H13-1: México. D.F., Secretaría de Programación y Presupuesto, Instituto Nacional de Estadística, Geografía e Informática, 1 mapa. http://mapserver.sgm.gob.mx/Cartas_Online/geologia/33_H13-1_GM.pdf
- Instituto Nacional de Estadística, Geografía e Informática (INEGI), 2022, Mapa Digital de México. <http://gaia.inegi.org.mx/mdm6/>
- Kennedy, J.F., Hawley, J.W., 2003, Late Quaternary paleohydrology of a linked pluvial-lake and ancestral Rio Grande system, Paso del Norte Region, southwestern USA and Northern Mexico, in XVI INQUA Congress, Paper No. 60-5: Geological Society of America Abstracts with Programs, 181.
- Kocurek, G., Ewing, R.C., 2005, Aeolian dune self-organization – implications for the formation of simple versus complex dune-field patterns: *Geomorphology*, 72(1-4), 94 – 105. <https://doi.org/10.1016/j.geomorph.2005.05.005>
- Kocurek, G., Carr, M., Ewing, R., Havholm, K.G., Nagar, Y.C., Singhvi, A.K., 2007, White Sands Dune Field, New Mexico: Age, dune dynamics and recent accumulations: *Sedimentary Geology*, 197, 313-331. <https://doi.org/10.1016/j.sedgeo.2006.10.006>
- Lancaster, N., 1983, Controls of dune morphology in the Namib sand sea: *Developments in Sedimentology*, 38, 261-289. [https://doi.org/10.1016/S0070-4571\(08\)70799-4](https://doi.org/10.1016/S0070-4571(08)70799-4)
- Lancaster, N., 1988, Controls of aeolian dune size and spacing: *Geology*, 16(11), 972 – 975. [https://doi.org/10.1130/0091-7613\(1988\)016<0972:COEDSA>2.3.CO;2](https://doi.org/10.1130/0091-7613(1988)016<0972:COEDSA>2.3.CO;2)
- Lancaster, N., 1989, Star dunes. *Progress in Physical Geography: Earth and Environment*, 13(1), 67-91. <https://doi.org/10.1177/030913338901300105>
- Lancaster, N., 1995, *Geomorphology of desert dunes*. New York, Routledge.
- Lancaster, N., 1999, Geomorphology of desert sand seas, in Goudie, A.S., Livingstone, I., Stokes, S. (Eds.), *Aeolian Environments, Sediments and Landforms*: Chichester, John Wiley & Sons, 49-70.
- Lancaster, N., 2022, Sand seas and dune fields, in Shroder, J.F. (Ed.), *Treatise on Geomorphology*, 2nd ed: MA, USA, Academic Press, Cambridge, 520- 539. <https://doi.org/10.1016/B978-0-12-818234-5.00127-9>
- Lancaster, N., Hesp, P. (Eds.), 2020, *Inland Dunes of North America*: Cham, Springer International Publishing, *Dunes of the World*. <https://doi.org/10.1007/978-3-030-40498-7>
- Langford, R.P., 2000, Nabkha (coppice dune) fields of south-central New Mexico, USA:

- Journal of Arid Environments, 46(1), 25-41. <https://doi.org/10.1006/jare.2000.0650>
- Langford, R.P., 2003, The Holocene history of the White Sands dune field and influences on eolian deflation and playa lakes: *Quaternary International*, 104(1), 31–39. [https://doi.org/10.1016/S1040-6182\(02\)00133-7](https://doi.org/10.1016/S1040-6182(02)00133-7)
- Langford, R.P., Rose, J.M., White, D.E., 2009, Groundwater salinity as a control on development of eolian landscape: An example from the White Sands of New Mexico: *Geomorphology*, 105(1-2), 39–49. <https://doi.org/10.1016/j.geomorph.2008.01.020>
- Lawton, T.F., Uruña, J.E.R., Solari, L.A., Terrazas, C.T., Juárez-Arriaga, E., Ortega-Obregón, C., 2018, Provenance of Upper Triassic–Middle Jurassic strata of the Plomosas uplift, east-central Chihuahua, Mexico, and possible sedimentologic connections with Colorado Plateau depositional systems, in Ingersoll, R.V., Lawton, T.F., Graham, S.A. (Eds.), *Tectonics, Sedimentary Basins, and Provenance: A Celebration of the Career of William R. Dickinson*: Geological Society of America Special Paper, 540, 481-507. [https://doi.org/10.1130/2018.2540\(22\)](https://doi.org/10.1130/2018.2540(22))
- Lorenz, R.D., Zimbelman, J.R., 2014, Fictional Dune Worlds. In: Lorenz, R.D., Zimbelman, R.E. (Eds.), *Dune Worlds*. Berlin, Springer Praxis Books, 283- 286. https://doi.org/10.1007/978-3-540-89725-5_
- McKee, E.D., 1966, Structures of dunes at White Sands National Monument, New Mexico (and comparison with structures of dunes from other selected areas): *Sedimentology*, 7, 3–69. <https://doi.org/10.1111/j.1365-3091.1966.tb01579.x>
- McKee, E.D., 1979, Introduction to a study of global sand seas, in McKee, E.D. (Ed.), *A study of global sand seas*: United States Geological Survey Professional Paper 1052, 3 - 19. <https://doi.org/10.3133/pp1052>
- McKee, E.D., Breed, C.S., Fryberger, S., Gebel, D., McCauley, C., 1974, *A Synthesis of Sand Seas Throughout The World*. Report to NASA Goddard Space Flight Center. <https://ntrs.nasa.gov/citations/19740022570>, accessed 1 August 2023.
- Nield, J.M., Baas, A.C.W., 2007, Investigating parabolic and nebkha dune formation using a cellular automaton modelling approach. *Earth Surface Processes and Landforms*, 33(5), 724–740. <https://doi.org/10.1002/esp.1571>
- Prospero, J.M., Ginoux, P., Torres, O., Nicholson, S.E., Gill, T.E., 2002, Environmental characterization of global sources of atmospheric soil dust identified with the Nimbus-7 total ozone mapping spectrometer (TOMS) absorbing aerosol product: *Reviews of Geophysics*, 40(1), 1002. <https://doi.org/10.1029/2000RG000095>
- Reeves, C.C., 1969, Pluvial Lake Palomas, northwestern Chihuahua, Mexico. *New Mexico Geological Society Guidebook*, 20, 143 – 154. <https://doi.org/10.56577/FFC-20.143>
- Rueda-Torres, J.R., Leon-Pesquiera, L.D., Gatica-Colima, A.B., 2022, Fabaceas del Área de Protección de Flora y Fauna Médanos de Samalayuca, Chihuahua, México: *Polibotánica*, 53, 1 - 12. <https://doi.org/10.18387/polibotanica.53.1>
- Sanchez, J.P., 2017, *La Ruta de Oñate: Early Parages of Northern Chihuahua and Southern New Mexico along the Camino Real de Tierra Adentro*: *Southern New Mexico Historical Review*, 24, 11-24.
- Sanchez, E.C., Esparza-Ponce, H., Díaz, C., Saenz, E., Boone, K., 2007, Use of Samalayuca dune sand on glass and ceramics processes: *American Ceramic Society Bulletin*, 86(4), 61-65.
- Schmidt, R.H. Jr., Marston, R.A., 1981, Los Medanos de Samalayuca, Chihuahua, Mexico. *New Mexico: Journal of Science*, 21(2), 21 – 27.
- Scuderi, L.A., Laudadio, C.K., Fawcett, P.J., 2010, Monitoring playa lake inundation in the western United States: Modern analogues to

- late-Holocene lake level change: Quaternary Research, 73(1), 48- 58. <https://doi.org/10.1016/j.yqres.2009.04.004>
- Secretaría de Medio Ambiente y Recursos Naturales (SEMARNAT), 2013, Programa de Manejo Área de Protección de Flora y Fauna Médanos de Samalayuca. Secretaria de Medio Ambiente y Recursos Naturales. https://simec.conanp.gob.mx/pdf_libro_pm/33_libro_pm.pdf (Accessed 30 June, 2023)
- Servicio Geológico Mexicano (SGM), 2003, Carta Geológico-Minera Escala 1:250,000 Cd. Juárez H13-1, Chihuahua. http://mapserver.sgm.gob.mx/Cartas_Online/geologia/33_H13-1_GM.pdf (Accessed 3 August, 2023).
- Sharp, R.P., 1966, Kelso Dunes, Mojave Desert, California: Geological Society of America Bulletin, 77(10), 1045 – 1074. [https://doi.org/10.1130/0016-7606\(1966\)77\[1045:KDMDC\]2.0.CO;2](https://doi.org/10.1130/0016-7606(1966)77[1045:KDMDC]2.0.CO;2)
- Valdez, A., Zimbelman, J.R., 2020, Great Sand Dunes, in Lancaster, N., Hesp, P. (Eds.), Inland Dunes of North America: Springer, Cham, 239–285. https://doi.org/10.1007/978-3-030-40498-7_7
- Vázquez Bernal, B.I., 2022, Las carreras de off-road y su correlación con el desierto de Samalayuca en Chihuahua, México: Chihuahua Hoy, 20, 295 - 318. <http://dx.doi.org/10.20983/chihuahuahoy.2022.20.11>
- Villegas, R.F., Flores, S.A., Morales, P., 1989, Caracterización hidrogeoquímica e isotópica del agua subterránea en la región de Villa Ahumada-Samalayuca, Estado de Chihuahua, México, in Estudios de Hidrología Isotópica en América Latina: International Atomic Energy Agency:Vienna, TECDOC-502, 399- 412.
- Webb, D.S., 1969, Facets of the geology of Sierra del Presidio area, North-central Chihuahua: New Mexico Geological Society Guidebook, 20, 182 – 185, <https://doi.org/10.56577/FFC-20.182>
- Werner, B.T., 1995, Eolian dunes: computer simulations and attractor interpretation: Geology, 23(12), 1107 – 1110. [https://doi.org/10.1130/0091-7613\(1995\)023<1107:EDCSAA>2.3.CO;2](https://doi.org/10.1130/0091-7613(1995)023<1107:EDCSAA>2.3.CO;2)
- Zheng, Z., Du, S., Taubenböck, H., Zhang, X., 2022, Remote sensing techniques in the investigation of aeolian sand dunes: A review of recent advances: Remote Sensing of Environment, 271, 112913. <https://doi.org/10.1016/j.rse.2022.112913>